Layer Structure Determination for Film Thickness Measurements of Thin HfO_2 Films Using X-ray Reflectivity and X-ray Photoelectron Spectroscopy

Yong-Qing Chang[1] and Wei-En Fu[2,#]

1 Rm.213, Bldg.8, 321, Sec. 2, Kuang Fu Rd., 30011, Hsinchu, Taiwan
2 Center for Measurement Standards, Industrial Technology Research Institute (ITRI)
Corresponding Author / E-mail: WeienFu@itri.org.tw, TEL: +886-3-573-2220, FAX: +886-3-572-4952

KEYWORDS : Thickness, HfO_2, SiO_2, ALD, XRR, XPS

As transistor feature sizes scaling down, the ultra-thin HfO_2 high-k dielectric has been used to replace SiO_2 for the gate dielectric for a better EOT. Grazing Incidence X-ray Reflectivity (GIXRR) is an accurate instrument to analyze the ultra-thin HfO_2 films based on an appropriate material model. However, the interfaces between layers of the ultra-thin HfO_2 films are not easily identified, especially when post-deposition annealing (PDA) process is applied. In this work, X-ray Photoelectron Spectroscopy (XPS) was used to evaluate the layer structures which were post-annealed up to 1000℃ using furnaces in the Ar ambiances. The experimental results and analysis showed that layer thicknesses, crystal phases and chemical structures of the ultra-thin HfO_2 films were significantly dependent on annealing temperatures. The structure analysis of the GIXRR spectra using the modified material structure model from the XPS analysis confirmed the interfacial broadening induced by the post-deposition annealing.

Manuscript received: January XX, 2011 / Accepted: January XX, 2011

1. Introduction

Grazing Incident X-Ray Reflectivity (GIXRR) has been frequently used to characterize ultra-thin HfO_2 films with an appropriate material structure model. However, the establishment of the material structure model is difficult, since structure change and interface stability induced by thermal annealing are critical issues in characterizing HfO_2 films using X-Ray Reflectivity (XRR) [1-3]. In this study, the HfO_2 films were evaluated by X-ray Photoelectron Spectroscopy (XPS) to obtain the layer structures induced by thermal annealing. Consequently, a modified material structure model based on the XPS evaluation is established in the GIXRR analysis.

The material structure model of the HfO_2 films was originally constructed as a three-layer model with a native oxide SiO_2 on Si-substrate [4] and a 10 nm HfO_2 layer on top. The top HfO_2 layer was atomic layer deposited (ALD) on an 8-inch p-type silicon wafer [5]. In order to investigate the layer structure change induced by annealing, the HfO_2 films were cut into 2x2 cm^2 and thermally annealed at 550 ℃, 850 ℃ and 1000 ℃ in Ar environments [5]. The inter-diffusion phenomenon of both as-deposited (ASD) sample and post-deposition annealing (PDA) films for accurate XRR fitting analysis was evaluated by the XPS. The obtained individual element XPS profiles at several different annealing temperatures were curve fitted to several annealing temperatures, which showed the composition changes of oxides and the layer structures of the films. Consequently, to analyze the obtained XRR spectra, a four-layer material model of HfO_2 (low-density)/HfO_2/SiO_2/Si-substrate based on XPS analysis was constructed to improve fitting process with XRR genetic algorithm (GA) analysis [6]. As a result, the film thickness of the HfO_2 films with modified material structure models were obtained accurately.

2. Structure and Composition Analysis

2.1 XPD Crystalinity

Typical XRD spectra of 10 nm HfO_2 films are shown in Fig. 1. A broad diffraction peak can be observed around 2θ angle at 30° to indicate that crystallization starts at ASD for 10 nm HfO_2 films. It can also be found that major crystallization occurs at 450 °C. The crystallization is mixed with monoclinic and orthorhombic phases, since at lower annealing temperatures, both orthorhombic (1 1 1) phase at 30.68° and monoclinic (-1 1 1) at 28.62° and (1 1 1) at

31.92° can be observed. However, the intensity of the orthorhombic (1 1 1) phase at 30.68° decreases with increasing annealing temperatures. It indicates that the orthorhombic phase disappeared and the monoclinic phase becomes dominant with increasing annealing temperatures [7].

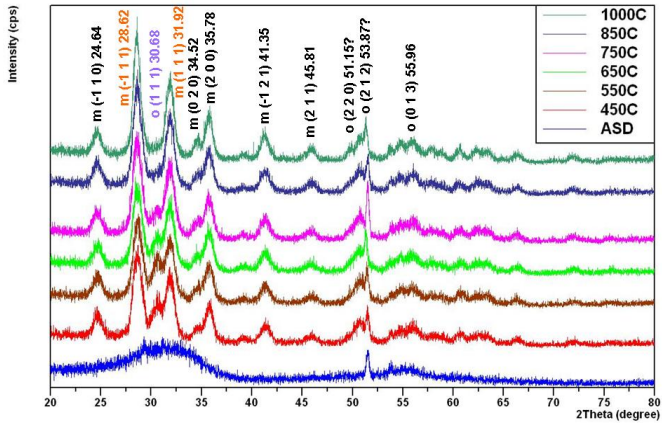

Fig. 1 XRD spectrum of ASD and PDA 10 nm HfO_2 films.

2.2 XPS Composition

Fig. 2 shows XPS surface-scans with well-defined Hf *4f*, O *1s* and Si *2p* peaks for ASD and PDA HfO_2 films. As shown in Fig. 2 (a), an obvious spin-orbit doublet can be identified for each spectrum and decomposed into two contributions of Hf $4f_{7/2}$ and Hf $4f_{5/2}$, at 17.10 eV and 18.70 eV, respectively, which are corresponding to oxide peaks. Another spin-orbit doublet can also be found at 15.75 eV and 14.30 eV, corresponding to Hf silicide, for the ASD films. The oxide peak shifts to higher BE in the vicinity of Si, i.e., to 17 ~ 17.5 eV, which can be attributed to $HfSi_xO_y$ [7]. At the low annealing temperature (~ 550 ℃), the core level of Hf *4f* shows a similar trend to that of the ASD film. The two peaks of the spin-orbit doublet are located at the BE of 16.90 eV and 18.60 eV with the splitting of 1.70 eV. However, as the annealing temperature increases, e.g. 850 ℃ and above, the two peaks of Hf $4f_{7/2}$ and Hf $4f_{5/2}$ shift to higher BE, such as (18.15 eV, 19.85 eV) for 850 ℃ and (18.25 eV, 19.95 eV) for 1000 ℃, respectively. The spin-orbit doublets split around 1.70 eV for the two spectra. The shift of the peaks to higher BE with increasing annealing temperatures is attributed to the formation of Hf silicates ($HfSi_xO_y$), which is mainly due to the changes occurring at the interface region [8].

Fig. 2 (b) shows the O *1s* XPS spectra for the ASD and PDA HfO_2 films at the indicated temperatures. A major peak can be fitted at 530.75 eV for the O *1s* XPS spectrum of the ASD film. This peak of the spectrum is attributed to the Hf-O bonding in HfO_2 [9]. When the film is annealed at 550 ℃ and above, a shoulder peak at higher binding energy side can be observed clearly appears. This peak shoulder can be fitted for an additional peak at 532.15 eV, which is corresponding to the Hf-O-Si bonding of the Hf silicate [8]. At high annealing temperatures (~ 850 ℃ and above), the peaks fitted at the shoulder shifted to higher BE, e.g. 533.15 eV, which is attributed to the Si-O bonding of the SiO_2. As a result, the Hf silicate formation can be formed from the interactions of HfO_x and SiO_x in an oxygen rich environment [10] at the high temperatures.

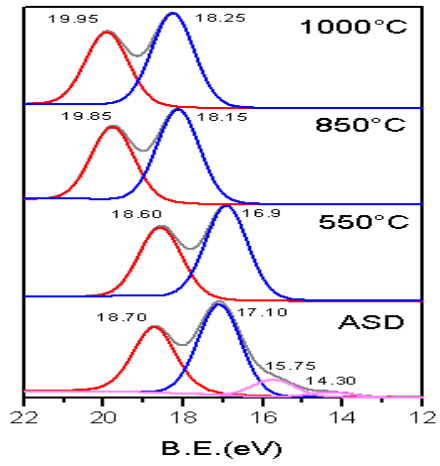

(a) Hf *4f*

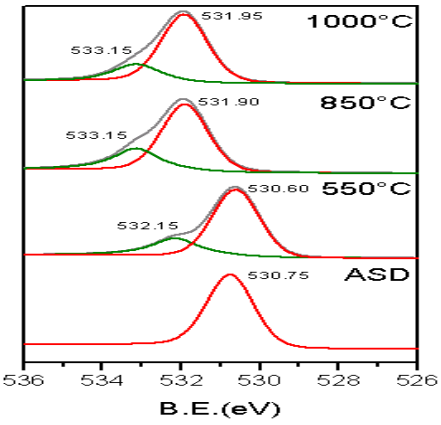

(b) O *1s*

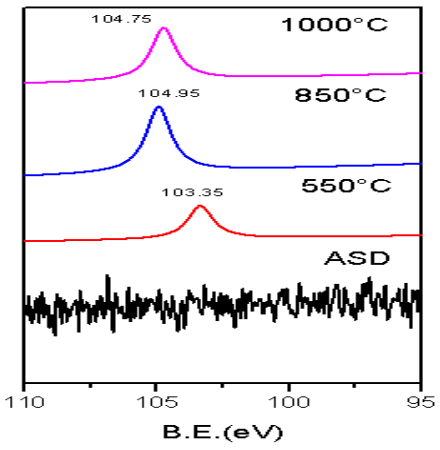

(c) Si *2p*

Fig. 2 XPS composition analysis (surface scan) of ASD and PDA 10 nm HfO_2 films: (a) Hf *4f* (b) O *1s* (c) Si *2p*.

A typical signal of core-level for Si *2p* is given in Fig. 2 (c) for 10 nm thickness HfO_2 films. Constrained by the XPS penetration depth, no detectable Si *2p*, is observed for the ASD film. As annealing temperatures increase to ~ 550 ℃, a major peak is observed for the PDA films. The peak is centered at 103.35 eV, which is corresponding to the $HfSi_xO_y$. Additionally, with increasing annealing temperatures, it can also be found that the peak is shifted to higher BE of ~ 104 eV. This shift to the higher BE are contributed from the formation of silicon oxide during the annealing. The observation of the $HfSi_xO_y$ and silicon oxide indicates that Si-O formation of the PDA films is

due to oxygen diffusion from the SiO_2 or HfO_2. As a result, the HfO_x and SiO_x are interacted to form $HfSi_xO_y$.

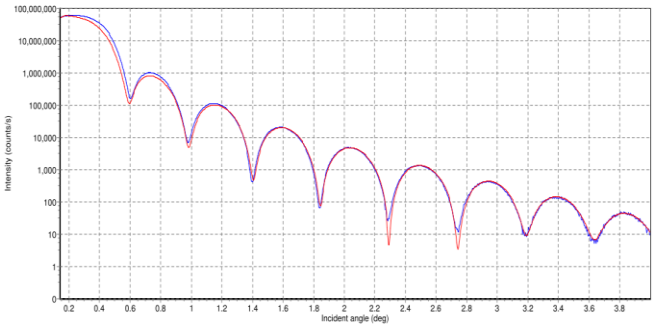

(a)

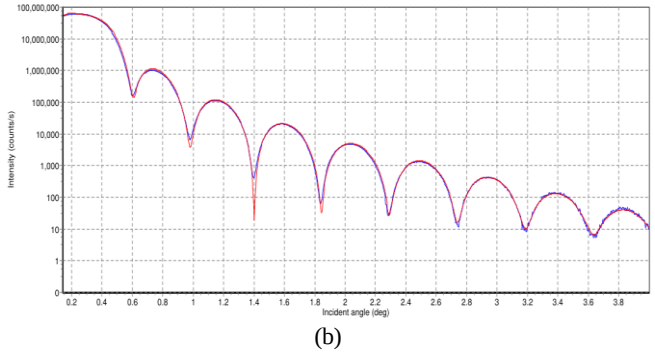

(b)

Fig. 3 XRR fitting spectrum of ASD HfO_2 10 nm films: (a) 3-layer model (b) 4-layer model.

3. XRR Fitting

GIXRR was primarily used to evaluate the thickness, surface roughness and interface stability for both ASD and PDA HfO_2 films. The layer structure analysis based on the XPS results is applied to modify the 3-layer material structure model (Fig. 3 (a)) in the analysis of GIXRR spectra. The interface broadening and generation of Hf silicate, according to the XPS analysis, are induced by thermal effects and thus increase the interfacial layer of thickness. Therefore the fitting accuracy can be improved by considering an extra layer to describe the Hf silicate at the interface between SiO_2/HfO_2 to form a 4-layer material structure model. While the surface contamination layer can be treated as a relatively low density HfO_2 layer with thickness around 1 nm at the upmost of HfO_2 films, which corresponds to a discrepancy at low incident angles of the GIXRR spectra (Fig. 3 (a)). Thus, an extra layer to describe the Hf silicate at the interface between SiO_2/HfO_2 or to describe the upmost contaminated layer has improved the overall match of the GIXRR profiles at the high annealing temperatures.

According to the 4-layer model fitting, as shown in Fig. 3 (b), thicknesses and interface properties of the HfO_2 films after the annealing process can be evaluated with consideration of Hf silicate or the low density HfO_2 layer at upmost.

The film thickness of the HfO_2 films are measured by X-ray Reflectivity (XRR) with theta-2theta scan in the range of omega = 0.14° to 4°. The fitting results for the density, thickness, surface roughness and interfacial roughness of the HfO_2 films before and after the annealing process are listed in Table 1. The fitting algorithm of the XRR software is based on the genetic algorithm (GA) analysis, which is a global optimization analysis for finding the neighborhood of global optimum, instead of the exact location of local minimum [6]. The fitting results (best fit value ~ 5) with the four-layer material structure model - HfO_2 (low-density)/HfO_2/SiO_2/Si-substrate, based on the XPS analysis, were improved dramatically, as shown in Fig. 3. With the material model obtained according to the XPS structure analysis, the XRR measurements provide accurate film thicknesses and layer evaluations.

4. Conclusions

The HfO_2 films with nominal thicknesses of 10 nm were deposited on p-type silicon (100) by ALD. According to the GIXRD analysis, significant crystallization appears at 450 ℃ and above, where the phases of crystallization structures are monoclinic and orthorhombic. As the annealing temperatures increase, the orthorhombic phase decreases and the monoclinic phases dominate at higher annealing temperatures. Based on the XPS analysis, the Hf silicate formation is contributed from the results of the interactions between HfO_x and SiO_x during deposition and annealing. The existence of $HfSi_xO_y$ broadens the interface with increasing annealing temperatures, and causes the increase of the interfacial layer thickness in the GIXRR analysis. As a result, the four-layer material structure model of HfO_2(low-density)/HfO_2/SiO_2/Si-substrate based on XPS analysis was constructed to significantly improve the XRR fitting process with genetic algorithm (GA).

Table 1 XRR fitting with a four-layer stack model.

HfO_2 (low-density)	ASD	550 ℃	850 ℃	1000 ℃
Density (g/cm^3)	1.8	1.6	1.4	1.4
Thickness (nm)	1.1	0.8	1.4	1.3
Roughness (nm)	0.5	0.3	0.3	0.5
HfO_2	ASD	550 ℃	850 ℃	1000 ℃
Density (g/cm^3)	10.3	10.5	9.8	9.5
Thickness (nm)	9.8	9.7	10.0	9.7
Roughness (nm)	0.4	0.4	0.4	0.4
SiO_2	ASD	550 ℃	850 ℃	1000 ℃
Density (g/cm^3)	2.5	2.7	2.6	2.7
Thickness (nm)	0.7	0.7	0.9	1.2
Roughness (nm)	0.3	0.3	0.6	0.6

ACKNOWLEDGEMENT

The financial support provided by the Bureau of Standards, Metrology and Inspection (BSMI) Nanometer-Scale Metrology Project is gratefully acknowledged.

REFERENCES

1. P.S. Lysaght, P.J. Chen, R. Bergmann, T. Messina, R.W. Murto, and H.R. Huff, "Experimental Observations of The Thermal Stability of High-k Gate Dielectric Materials on Silicon", J. of Non-Crystalline Solids, Vol. 303, pp. 54-63, 2002
2. C. Wiemer, S. Ferrari, M. Fanciulli, G. Pavia, and L. Lutterotti, "Texture, Residual Stress And Structural Analysis of Thin Films Using A Combined X-ray Analysis", Thin Solid Films, Vol. 450, pp. 34-41, 2004
3. M. Modreanu, J. Sancho-Parramon, O. Durand, B. Servet, M. Stchakovsky, C. Eypert, C. Naudin, A. Knowles, F. Bridou, and M.-F. Ravet, "Investigation of Thermal Annealing Effects on Microstructural And Optical Properties of HfO_2 Thin Films", Appl. Surf. Sci., Vol. 253, pp. 328-334, 2006
4. W.-J. Qi, R. Nieh, B. H. Lee, L. Kang, Y. Jeon, K. Onishi, T. Ngai, S. Banerjee, and J. C. Lee, "MOSCAP And MOSFET Characteristics Using ZrO_2 Gate Dielectric", Int. Electr. Devices Meeting. IEDM Technical Digest., pp. 145-148, 1999
5. H. Kim, H.-B.-R. Lee and W.-J. Maeng, "Applications of Atomic Layer Deposition to Nanofabrication And Emerging Nanodevices", Thin Solid Films, Vol. 517, pp. 2563-2580, 2009
6. A.D. Dane et al., "Application of Genetic Algorithms for Characterization of Thin Layered Materials by Glancing Incidence X-ray reflectometry", Physica B, Vol. 253, pp. 254-268, 1998
7. M.-H. Cho, Y.S. Roh, C.N. Whang, K. Jeong, S.W. Nahm, D.-H. Ko, J.H. Lee, N. I. Lee, K. Fujihara, "Thermal Stability And Structural Characteristics of HfO_2 Films on Si (100) Grown by Atomic-Layer Deposition", Appl. Phys. Lett., Vol. 81, pp. 472-474, 2002
8. S.J. Wang, P.C. Lim, A.C.H. Huan, C.L. Lu, J.W. Chai, S.Y. Chow, J.S. Pan, Q. Li, C.K. Ong, "Reaction of SiO_2 with Hafnium Oxide in Low Oxygen Pressure", Appl. Phys. Lett., Vol. 82, pp. 2047-2049, 2003
9. P. D. Kirsch, C. S. Kang, J. Lozano, J. C. Lee, J. G. Ekerdt, "Electrical And Spectroscopic Comparison of HfO_2/Si Interfaces on Nitrided And Un-nitrided Si (100)", J. of Appl. Phys., Vol. 91, pp. 4353-4363, 2002
10. T.P. Smirnova, L.V. Yakovkina, V.N. Kitchai, V.V. Kaichev, Yu.V. Shubin, N.B. Morozova, K.V. Zherikov, "Chemical Vapor Deposition And Characterization of Hafnium Oxide Films", J. Phys. Chem. Solids, Vol. 69, pp. 685-687, 2008